SECONDARY PHASES IN SPRAY DEPOSITED 2024-20Si-5Fe ALLOY①

Yuan Xiaoguang and Ren Luquan
*School of Agricultural Mechanical Engineering,
Jilin University of Technology, Changchun 130025, P. R. China*
Cui Chengsong, Xu Daming and Li Qingchun
*School of Materials Science and Engineering,
Harbin Institute of Technology, Harbin 150001, P. R. China*

ABSTRACT 2024-20Si-5Fe alloy has been prepared using spray deposition technology, and secondary phases in the alloy have been investigated. Si, $\delta(FeSi_2Al_4)$, $\beta(Fe_2Si_2Al_9)$ and $Al_8Si_6Mg_3Fe$ phases have been identified in the alloy. Primary silicon, eutectic silicon and δ phase exhibited a particle-like, flake-like and acicular morphology respectively. β phase came from the transformation of δ phase during hot extrusion and solution treatment. $Al_8Si_6Mg_3Fe$ phase exhibited a small particle-like morphology as well, and dispersed in the matrix.

Key words spray deposition Al-Si-Fe alloy secondary phase

1 INTRODUCTION

Rapid solidification (RS) is a new technology to prepare high property alloys, which can extend the solid solubility limit of alloy, suppress the formation of coarse and brittle phase, and promote the formation of metastable phase[1]. RS Al-Si-Fe-Cu-Mg alloy with a relatively low coefficient of thermal expansion (CTE), high wear resistance and good thermal stability has engendered considerable interest in this alloy family as candidate materials for high efficiency automobile engines and air conditioning compressors[2]. The main reasons of high mechanical properties in the alloy belong to the fine matrix, small Si phases, and especially disperse intermetallics[3, 4].

Differentiating the structure of the intermetallics in RS 2024-20Si-5Fe alloy is difficult because a large amount of alloying elements is included in it and they can form many kinds of intermetallics[5]. The reported results about the structure of intermetallics were quite inconsistent[3, 5]. Therefore, differentiating the structure of the intermetallics in the alloy is important for this alloy. The purpose of this paper is to investigate the type and morphology of secondary phases in the alloy prepared by spray deposition technology.

2 EXPERIMENTAL

The starting materials used in the present investigation were 2024 alloy with norminal composition (mass fraction, %, similarly hereinafter) Al-4.5Cu-1.6Mg-0.6Mn, magnesium ingot with 99.9% Mg, recrystallized silicon with 99.7% Si, and iron scrap with 99% Fe. The deposited preform had the composition of Al-20.8Si-5.4Fe-4.0Cu-1.0Mg. Spray deposition technology can be seen in Ref. [6]. Consolidation technology was hot extrusion at a temperature of 450 ℃, with a reduction ratio of 12∶1. Semi-finished product was shaped into rods with a diameter of 15 mm.

① Project 59605012 Supported by the National Natural Science Foundation of China
Received Nov. 27, 1997; accepted Apr. 13, 1998

The T6 temper treatment was applied, which consisted of solution treatment at 470 ℃ for 1.5 h followed by quenching in water, a natural ageing for 4 d and artificial ageing at 120 ℃ for 24 h.

Optical metallographic specimens were prepared using normal techniques, and etched with a specific Keller solution. Microstructure observations were performed using a Philips CM12/S transmission electron microscope (TEM) and an S-570 scanning electron microscope (SEM). The X-ray diffraction experiments were performed on O/MAX-RBX diffractometer using CuK_{α} radiation.

3 RESULTS AND DISCUSSION

Fig. 1 shows the X-ray spectrums of spray deposited 2024-20Si-5Fe alloy. The possible phases calibrated in the extruded alloy included $Al_8Si_6Mg_3Fe$, $\beta(Fe_2Si_2Al_9)$, $\delta(FeSi_2Al_4)$ and Si, and a small amount of Al_2CuMg phase may exist. After T6 temper, a new possible phase appeared, which may be $CuAl_2$. The quantity of β and $Al_8Si_6Mg_3Fe$ phase increased little after T6 temper. Si, δ and $Al_8Si_6Mg_3Fe$ phases had relatively high volume fractions in the extruded and T6 tempered alloy, so they were principal secondary phases in the alloy.

3.1 Silicon phase

For hypereutectic Al-Si alloy silicon phase can be divided into primary and eutectic phases[7]. Fig. 2 shows the microstructure of the alloy before and after T6 temper, which composes particle-like and short acicular morphology phases. The particle-like phase was identified using EDS, namely, primary Si phase. The formation of particle-like Si phase, however, may be attri-

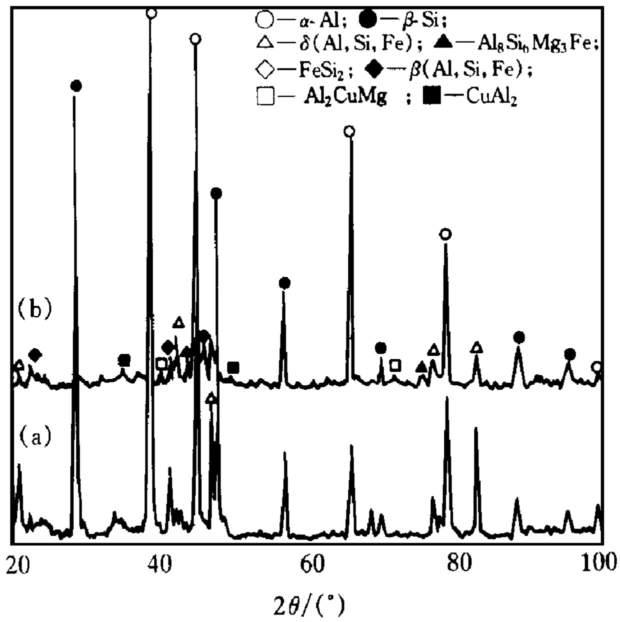

Fig. 1 X-ray spectrums of spray deposited 2024-20Si-5Fe alloy
(a) —Before T6 temper; (b) —After T6 temper

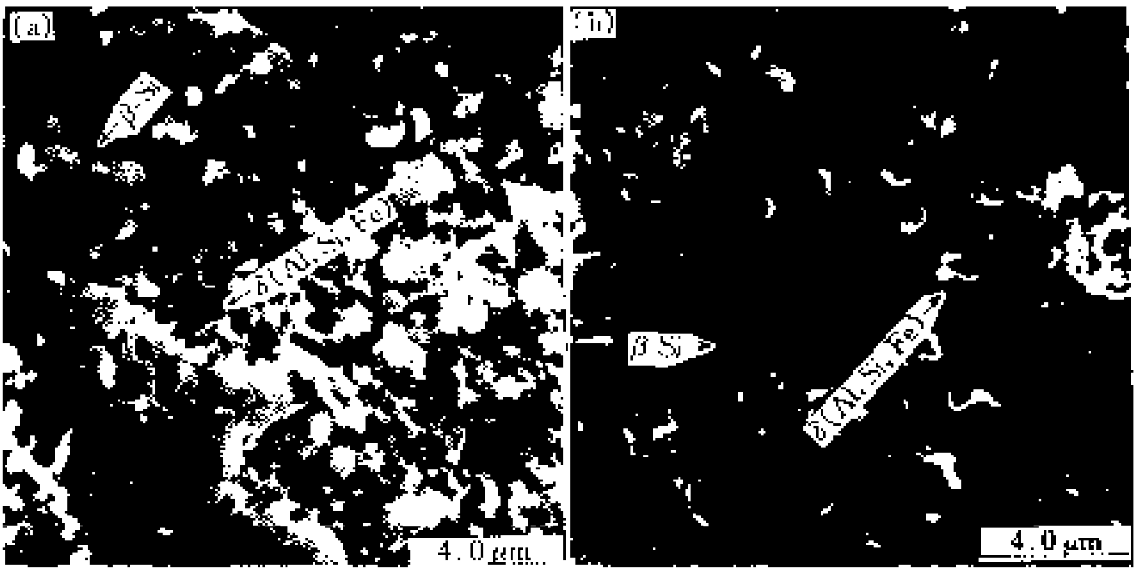

Fig. 2 SEM photographs of spray deposited 2024-20Si-5Fe alloy
(a) —Before T6 temper; (b) —After T6 temper

buted to three possible causes. First, the relatively high cooling rates present during deposition ($2.0\times10^3\sim4.6\times10^3$ K/s[8]) may effectively alter the morphological stability of the Si phase[9]. Second, the repeated deformation and fracture experienced by the partially solidified droplets during deposition may effectively break the Si phase that formed prior to the deposition stage[6]. Third, the extrusion process can break the wedges of Si phase to make the phase granulate. Comparing Fig. 2a with Fig. 2b, T6 temper treatment canceled the wedges of Si phase making the particle-like phase more round, but no coarsening.

Fig. 3 shows the morphology of flake-like Si phase named eutectic Si phase. Compared with the casting Al-Si binary alloy[10], the eutectic Si phase was effectively refined. The tip of flake-like Si phase after T6 temper (Fig. 3b) was more round than that in extruded alloy, which had the same change as primary Si phase.

3.2 (Al, Si, Fe) Ternary pahse

(Al, Si, Fe) ternary phases in the alloy have two possible structures, β and δ. $\alpha(Fe_3SiAl_{12})$ can not appear for the high silicon composition[7] and high cooling rate[11]. The short acicular phases in Fig. 2 were identified using EDS containing Al, Fe and Si elements with an atom ratio of Al∶Fe∶Si ≈ 4∶1∶2, they may be δ phases. δ phase is a metastable phase that forms hardly at IM conditions because it will change into β phase with the reduction of temperature[7]. In the spray deposited preform of the same alloy, β phase was not identified[12]. It is shown that relatively high cooling rates effectively depressed the transformation of metastable δ to equilibrium β phase during spray deposition. Therefore, it can be deduced that β phase formed during hot extrusion and T6 temper. Moreover, the diffraction intensity of δ phase being higher than that of β phase in the extruded and T6 tempered alloy proved that δ phase had a better thermal stability.

Fig. 4 shows a typical morphology of (Al, Si, Fe) ternary phase in the extruded alloy. It can be seen that (Al, Si, Fe) ternary phase had a similar morphology as in casting alloy[7], but it was broken and refined. According to the symmetry characteristic of electron diffraction spots

Fig. 3 TEM photographs of eutectic Si phase in spray deposited 2024-20Si-5Fe alloy
(a) —Before T6 temper; (b) —After T6 temper

Fig. 4 Morphology of δ($FeSi_2Al_4$) phase before T6 temper

(see Fig. 5), these electron diffraction patterns would belong to pyramidal system, not belong to clinorhombic system. So, (Al, Si, Fe) ternary phase in the extruded alloy had δ phase structure.

Fig. 6 shows the morphology of (Al, Si, Fe) ternary phase after T6 temper. The characteristics of electron diffraction pattern proved that (Al, Si, Fe) ternary phase had the structure of δ phase as well. Compared with before T6 temper, δ phase was more round, which can be attributed to the granulation caused by solution treatment.

Although β phase was identified using XRD in the T6 tempered alloy, it could not be observed using electron microscope. This may be attributed to two possible causes. First, the volume fraction of β phase that came from the transformation of δ phase was very small, and its morphology was very fine. Second, the partial transformation of δ phase to β phase resulted in δ phase and β phase scrambling together. So, it is difficult to distinguish β phase from δ phase. The above results were similar to those in the alloy prepared by RS gas atomization[5] and two-stage atomization[13].

3.3 Other phases

Besides Si and (Al, Si, Fe) ternary phases, a small amount of other secondary phases was also observed at the interdendritic boundaries. This is evidenced by the bright-field TEM microscope shown in Fig. 7, which reveals the presence of secondary phase along the interdendritic boundaries of the α-Al phase. This phase was identified using electron diffraction to be $Al_8Si_6Mg_3Fe$ which belongs to hexagonal system.

The distribution of $Al_8Si_6Mg_3Fe$ phase in the matrix before and after T6 temper is shown in Fig. 8. After T6 temper (Fig. 8b), this phase distributed inside grains and at grain boundaries with an average size of 0.13 μm, which has the characteristic of precipitation phase. Compared with before T6 temper (Fig. 7 and Fig. 8a), $Al_8Si_6Mg_3Fe$ phase had an increased volume fraction, exhibited a more round morphology, and coarsened little. Therefore, a large amount of precipitation phases in the alloy was the main reason that the tempered alloy possessed much higher mechanical properties than the extruded alloy[12]. The fact that large dislocations were

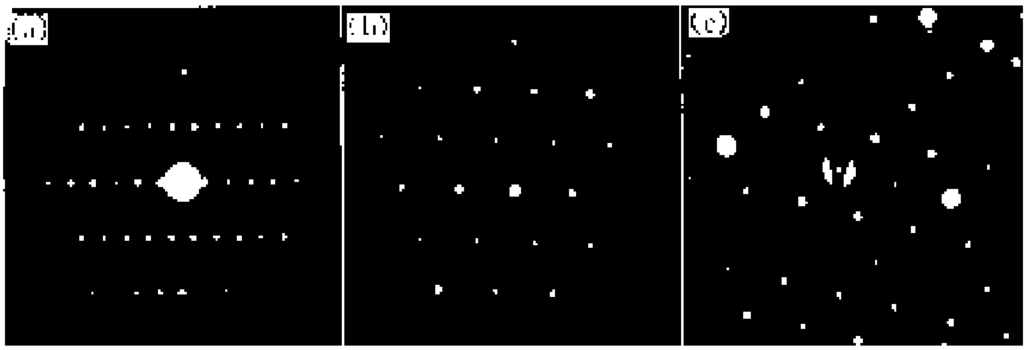

Fig. 5 Electron diffraction patterns of δ($FeSi_2Al_4$) phase
(a) —Zone axis[112]; (b) —Zone axis[003]; (c) —Zone axis[110]

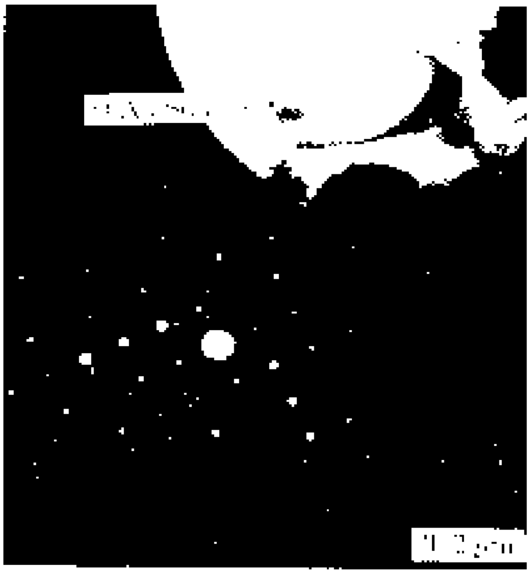

Fig. 6 Morphology and electron diffraction patterns of δ($FeSi_2Al_4$) phase after T6 temper

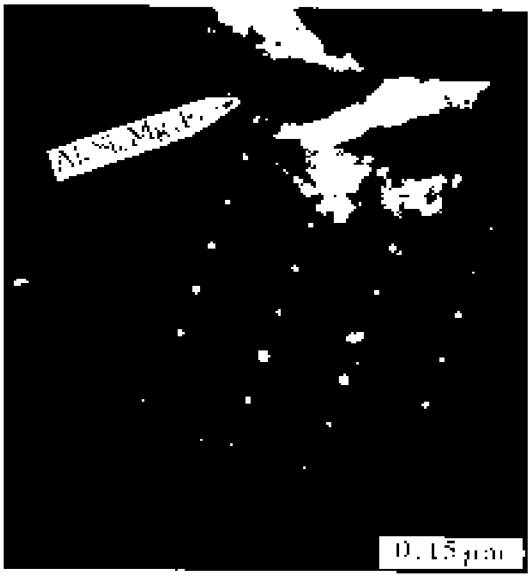

Fig. 7 Morphology and electron diffraction patterns of $Al_8Si_6Mg_3Fe$ phase before T6 temper

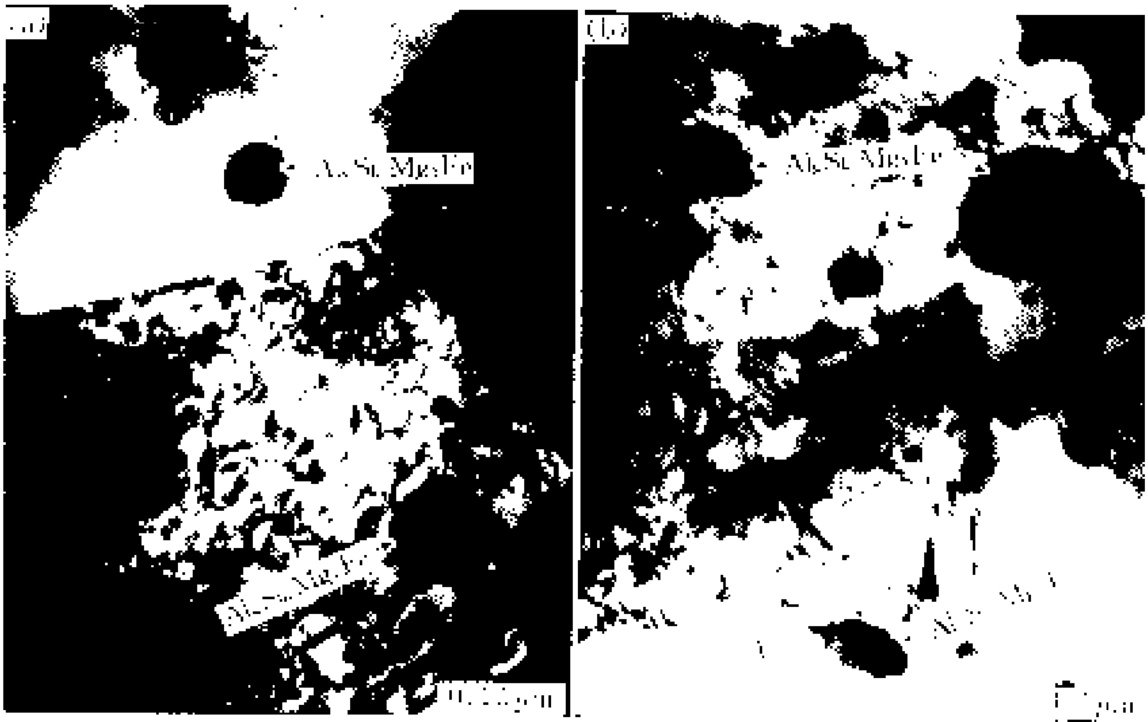

Fig. 8 Distribution of $Al_8Si_6Mg_3Fe$ phase in matrix
(a) —Before T6 temper; (b) —After T6 temper

around $Al_8Si_6Mg_3Fe$ phase (Fig. 8b) and little recrystallization structure appeared in the area of low intensity dislocation (Fig. 8b, *A* area) proved the effects on strengthening matrix and depressing recrystallzation. In addition, the good thermal stability of the precipitation phase $Al_8Si_6Mg_3Fe$ phase was one of the reasons that the alloy possessed a higher elevated strength than RS Al-Si-Cu-Mg alloy with precipitation phase of Al_2CuMg[14].

Possible phases Al_2CuMg and Al_2Cu identified by XRD can not be confirmed using TEM. This may be attributed to their very small volume fractions and sizes.

4 CONCLUSIONS

(1) The principal secondary phases in the 2024-20Si-5Fe alloy prepared by the spray deposition technology included Si, β($Fe_2Si_2Al_9$), δ ($FeSi_2Al_4$) and $Al_8Si_6Mg_3Fe$ phase.

(2) The primary Si phase exhibits a particle-like and small size morphology. The eutectic Si phase exhibits a flake-like morphology. T6 temper causes the granulation of Si phases, but no coarsening.

(3) Principal (Al, Si, Fe) ternary phase has the metastable structure of δ phase with an acicular morphology. Little equilibrium β phase comes from the partial transformation of δ phase during hot extrusion and T6 temper.

(4) $Al_8Si_6Mg_3Fe$ phase exhibits a small particle-like morphology in the matrix of the alloy. T6 temper causes the increasing of volume fractions of β(FeSiAl) and $Al_8Si_6Mg_3Fe$ phase.

REFERENCES

1 Lavernia E J, Ayers J D and Srivatsan S. International Materials Reviews, 1992, 35(1): 20.

2 Sumitomo Light Metal Industries Ltd. Metal Powder Report, 1994, 49(1): 26.

3 Mocellin A, Fougeres R and Gobin P F. J Mater Sci, 1993, 28: 4855.

4 Mocellin A, Brechet Y and Lavernia E J. Acta Metall Mater, 1995, 43(3): 1135.

5 Zhou J and Duszozyk J. J Mater Sci, 1992, 27: 3856.

6 Yuan X G. PhD Dissertation, (in Chinese). Harbin: Harbin Institute of Technology, 1997: 26.

7 Monldofo L F. Aluminum Alloys, Structure and Properties. London: Butterworth, 1976: 759.

8 Cui C S. PhD Dissertation, (in Chinese). Harbin: Harbin Institute of Technology, 1994: 36.

9 Wu Y, Cssada W A and Lavernia E J. Metall and Mater Trans, 1993, 23: 1235.

10 Kumar J, Sivaramakrishnan C C, Mahanti R K *et al*. Aluminium, 1977, 53(6): 361.

11 Zhou J, Duszczyk J and Korevaar B M. J Mater Sci, 1991, 26: 3041.

12 Yuan X G, Xu D M and Li Q C. Acta Metallurgica Sinica, (in Chinese), 1997, 33(3): 248.

13 Yuan X G, Xu D M and Li Q C. Acta Metallurgica Sinica, (in Chinese), 1996, 32(10): 1034.

14 Zhou J and Dusczyk J. In: Exner H E and Schumacher V eds, Proceedings of the First European Conference on Advanced Materials and Processe: Vol Ⅰ. West Germany, 1990: 241– 248.

(Edited by Peng Chaoqun)